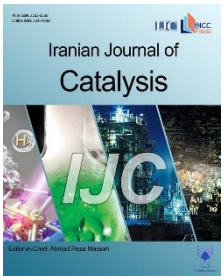

Volume 15, Issue 4, (2025) Article (1-13)

Iranian Journal of Catalysis (IJC)

https://doi.org/10.57647/j.ijc.2025.1504.43

Preparation of Iron Catalysts on Reliable Gamma Alumina Supports for Fischer-Tropsch Synthesis

Kousar Dinarvandi[1], Mozhgan Zakeri[1,*], Hossein Atashi[1], Ali Akbar Mirzaei[2]

[1] *Department of Chemical Engineering, Faculty of Engineering, University of Sistan and Baluchestan, Zahedan, Iran*
[2] *Department of Chemistry, University of Sistan and Baluchestan, Zahedan, Iran*

***Corresponding author:** m_zakeri@eng.usb.ac.ir

Original Research

Received:
21 February 2025

Revised:
30 May 2025

Accepted:
16 September 2025

Published online:
26 October 2025

Published in issue:
31 December 2025

Abstract

In addition to high activity, a reliable catalyst must exhibit resistance to thermal and mechanical stresses, which is achieved through high mechanical strength. In this work, nine samples of γ-alumina catalyst supports were prepared using the oil-drop method according to the Taguchi M9 design. To assess the reliability of the supports, all samples were evaluated through mechanical strength testing. Iron catalysts were then prepared on these supports via the wet impregnation method for use in Fischer-Tropsch synthesis. The results revealed that the catalyst prepared on the support with the following specifications: An Al/H ratio of 1.8, a hexamethylenetetramine solution concentration of 30 wt.%, an aging time of 12 hours, and a calcination temperature of 650°C, demonstrated good conversion in addition to relatively high mechanical strength (65 MPa), among the other samples. Finally, this reliable catalyst was evaluated in a reactor to determine the optimal conditions for achieving higher conversion and selectivity. The best results for CO conversion (61.9%) and C_4 selectivity (4.1%) were obtained when the reaction operational conditions were T=270°C, P=3bar, GHSV=2153.40 h^{-1}, and H_2/CO=1

Keywords: Fischer–Tropsch synthesis; Mechanical strength; Oil drop method; Reliable catalyst; Selectivity modelling

1. Introduction

The performance of solid catalysts strongly depends on the type of catalyst support and even its synthesis method [1,2]. Supports such as Al_2O_3, SiO_2, TiO_2, and zeolites play a vital role in controlling metal dispersion [3-5]. γ-alumina is the most widely used commercial catalyst support due to its high specific surface area, desirable pore structure, and excellent chemical and thermal stability, which enhance the performance of modern catalysts and adsorbents [6]. The synthesis method, and especially the method of forming the support of solid catalysts, strongly influences the structural properties of the catalysts made based on them. One of the essential structural properties of solid catalysts on an industrial scale is mechanical strength. It is obvious that a reliable industrial catalyst, in addition to having good catalytic performance, must have high mechanical strength so that it does not undergo rapid failure and erosion when faced with mechanical, thermal, and chemical stresses inside the reactor and has a longer lifetime [7,8]. To date, γ-Al_2O_3 support has been synthesized via several chemical methods, including sol-gel [9], spray drying [10,11], snowball granulation, extrusion [12], tableting [13], and oil–drop [14]. The products of spray-drying are in powder form with a particle size of less than 0.1 mm. In general, the catalysts made with this method were used in slurry phase reactors and fluidized bed reactors [15]. Tableting and extrusion usually have enough strength, whereas syntheses of granules with the snowball method, in addition to low strength, particle sizes, and spheres are random and irregular [16]. The spherical shape of the catalyst supports, produced by the oil-drop method, exhibits high mechanical strength, uniformity in size, and a large surface area [11]. Furthermore, the spherical

geometry of the support in moving beds provides good mobility, minimizes attrition and breakage due to collision in packed beds, and results in a lower pressure drop [14]. M. Abdollahi et al. [1] investigated the effect of operating variables on the structural and textural properties of γ-alumina granules produced via the oil-drop route. The results of this research showed that the increase in calcination temperature led to both an increase in mean pore diameter and a decrease in the total surface area. However, the crush strength increased as well. A. Islam et al. [14] prepared spherical γ-alumina granules by an oil drop granulation process. It was observed that the ejected liquid with relatively high surface tension and low viscosity formed a spherical droplet, which had very high mechanical strength after calcination.

The Fischer-Tropsch synthesis (FTS) is a well-established catalytic process in the synthesis of liquid hydrocarbons from gaseous feedstock and syngas that can be derived from various non-petroleum carbon resources, such as coal, natural gas, biomass [17-21]**.**
The objective of the present work is the preparation of reliable γ-alumina supports for the synthesis of γ-alumina-supported iron catalysts by the oil-drop method. The main parameters that affected the essential properties of the support were assessed. The γ-alumina granule supports were characterized by XRD, BET, SEM, EDS analyses, and mechanical strength tests for reliability assessment.

Then, iron-based catalysts were synthesized using the wet impregnation method of optimally synthesized supports, and evaluated in terms of CO conversion and product selectivity under different FTS conditions in a fixed-bed microreactor.

2. Materials and methods

2.1. Materials

The gamma-alumina (γ-Al_2O_3) supports were prepared using the oil-drop method. Aluminum powder (purity of 99.98% and an average particle size of <100 μm), hydrochloric acid (37 wt .%, Merck), and hexamethylenetetramine (HMTA, 99 wt. %, Merck) were used as raw materials. The synthetic oil (Gulf Fidelity PAO-100) has been selected for the synthesis process. The deionized water was used in all synthesis and washing processes.

2.2. Design of experiments

The Taguchi design performance, to increase the reliability of responses, provides information about the effect of several factors and their interaction with a minimum number of experiments at once [22]. The Taguchi M9 design was used to investigate the effects of the variables on the surface area and mechanical strength of synthesized γ-alumina supports by the oil-drop method and to optimize the synthesis conditions. It is necessary to explain further that for reasons reduction of material cost and time in depositing iron metal on the catalyst support, the Taguchi M9 design method was used with a smaller number of tests (9 tests). Table 1 shows the selected three levels for the four factors**.**

Table 1. The investigated variables and their levels

Variables	Code	Levels		
(mol Al/mol H)	P1	1.6	1.8	2
Aging time in hot oil (hr)	P2	4	8	12
HMTA solution concentration (wt. %)	P3	30	35	40
Calcination temperature (°C)	P4	550	650	750

2.3. Synthesis of alumina hydrosol

The alumina hydrosol samples were prepared based on the experimental design shown in Table 1. Initially, hydrochloric acid (HCl) was slowly added to 300 mL of deionized water. After that, 20 gr of aluminum powder was added to this solution in several stages at a temperature of 67 ◦C and under vigorous stirring. Finally, after the complete dissolution of the aluminum powder and the evaporation of excess water, the final aluminum content in the hydrocel alumina was adjusted to 13 wt. %.

2.4. Preparation of spherical γ-alumina supports

In this work, γ-alumina supports were prepared using the oil drop method, as described in previous work from this research team [1]. At first, 50 mL of alumina hydrosol was mixed with 100 mL of HMTA aqueous solution (30 wt. %) at 10°C under vigorous stirring for 5 min to create a uniform solution. The prepared sol was injected dropwise into an oil column at a temperature of approximately 85 ± 1 °C to form a gel. At this stage, the hydrolysis process begins, and the surface tension created along the oil column results in spherical wet gel droplets. The spherical gelled droplets were removed from the bottom of the oil column after a 12 h aging period and treated in an ammonium hydroxide solution with a concentration in the range of about 8 wt. % for 3hr at 60℃. Then, the white alumina spherical samples were carefully washed with deionized water and ethanol. The obtained granules were placed in an ethanol solution for a few days to minimize shrinkage during the drying step. Finally, the spherical granules were dried at room temperature for 24 h and calcined at 650 °C for four h at a low rate of 2℃/min to avoid damage to the granules. Figure 1 shows the experimental setup used for the synthesis of γ-alumina spherical samples.

2.5. The mechanical strength assessment

The mechanical strength evaluation of the synthesized granule supports was measured according to the ASTM D-4179-01 by a universal testing machine (model 4206, Instron, USA). The mechanical strength was calculated by using the equation below [23]:

$$\text{Fracture strength} = \frac{F_b}{\pi R^2} \quad (1)$$

Where F_b is the maximum force leading to fracture and R is the radius of the nondeformed granules.

2.6. Catalyst preparation

The catalyst samples were prepared by the wet impregnation method in three steps. First, γ-AL_2O_3 granule support samples were soaked in ethanol.

After soaking, the supports were placed in a 2.5M of Fe $(NO_3)_3.9H_2O$ (99% Merck) as the precursor and heated at 50℃ for 2 h in an oven. Then, the samples were dried at 80℃ for 12 h to give a material denoted as the catalyst precursor and calcined at 500 ℃ For 6 hr to produce the final catalyst. The loading of the Fe metal was carried out in two wet impregnation steps**.** After the second impregnation /drying/calcination step, certain amounts of KNO_3 and Cu $(NO_3)_2$ as K and Cu promoters were added to the previous catalysts with impregnation. In general, K and Cu as chemical promoters improved the FTS activity. After K and Cu addition, the samples were dried and calcined again using the same conditions as used formerly.

2.7. Catalyst Characterizations

Identifying the crystal phases and the extent of dispersion of the active species in this test was carried out using X-ray diffraction (M18XHF-SRA, Mac Science) patterns with nickel-filtered Cu Ka (λ=1.54056 Å) radiation over the range of 2θ from 20 to 80°, at a scanning speed of 1° min-1.

The specific surface area of the spherical γ-alumina supports was determined by the Brunauer, Emmett, and Teller (BET) method. In the BET analysis, before measurement, each support sample was degassed under a nitrogen atmosphere at 300k for 5hr and then evacuated at 77.35 k for 90 min. Scanning electronic microscopy (SEM, JEOL JSM7401, Japan) was used to observe the morphology and size of the optimgamma-aluminasample and catalyst (before and after the test) with an accelerating voltage of 1500 kV. Energy dispersive X-ray analysis (EDX) is an X-ray technique applicable to identifying the elemental composition of materials.

In addition, the crushing strength of the γ-alumina catalyst sample was measured using a universal testing machine (model 4206, Instron, USA) under a quasi-static compressive loading rate of 0.5 mm/min.

Figure 1. Several photographs of the spherical γ-alumina supports preparation steps

2.8. Catalyst FTS test

The experiments were carried out in a fixed-bed microreactor (Figure 2). The inlet gas combination, comprising 99.99% purity (H_2, CO), served as the feed for the reactor and was passed through pressurized cylinders using mass flow controllers (MFC). After adjusting the volume flow rates of H_2 and CO, the gases were transferred into the mixing chamber through the needle valves to be uniformly fed into the reactor bed. The furnace temperature is controlled by a digital controller. The total pressure is regulated using a back pressure regulator (PBR). In the gas chromatography (GC) device, gases and product gases were analyzed for CO and C hydrocarbons in two sections: the thermal conductivity detector (TCD) and the flame ionization detector (FID), utilizing helium as a carrier gas. Before the reaction, in each test, 2.0 g of the catalyst was reduced at atmospheric pressure under a flow of pure hydrogen (GHSV=3000 h^{-1}) for 12 hr at 400°C. After reduction, the FTS reaction tests were performed on each of the nine catalyst samples under the same experimental conditions within the following ranges: temperature 240-300°C, pressure= 2 bar, H_2/CO molar ratio of 2/1, and GHSV= 3000 h^{-1}. Results are presented in terms of CO conversion and hydrocarbons selectivity as follows (equations 2-4):

$$\text{CO conversion (\%)} = \frac{\text{CO}_{\text{in}} - \text{CO}_{\text{out}}}{\text{CO}_{\text{in}}} \times 100 \quad (2)$$

$$\frac{\text{O}}{\text{P}}\ \text{selectivity (\%)} = \frac{\text{moles of (ethylene + propylene)}}{\text{moles of (methane + propane + } \text{C}_4 + \text{C}_5)} \times 100 \quad (3)$$

$$\text{C}_\text{i}\ \text{hydrocarbon selectivity (\%)} = \frac{\text{moles of C}_\text{i}}{\text{total moles}} \times 100 \quad (4)$$

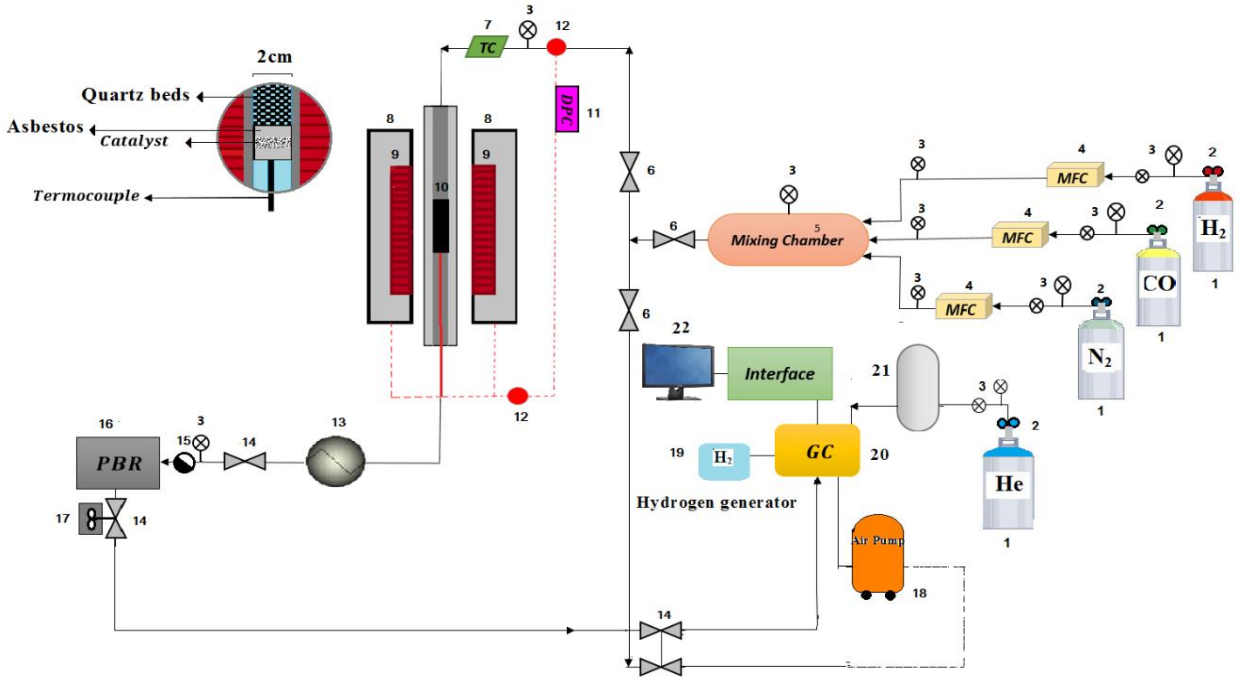

Figure 2. The experimental schematic of the fix-bed reactor in Fischer -Tropsch synthesis over iron based catalyst.1-gas cylinders, 2- pressure regulators, 3- pressure gauge, 4- mass flow controller (MFC), 5- mixing chamber 6- ball valves 7- temperature controller (TC), 8- tubular furnace, 9- temperature indicators, 10- reactor bed, 11- temperature digital program controller, 12- resistance temperature controller,13- condenser, 14- valve, 15- trap,16- back pressure regulator(PBC),17- control panel ,18-air pump,19- hydrogen generator, 20- gas chromatograph (GC), 21- silica gel column, 22- conductivity detector (TCD) and flame ionization detector (FID)

3. Results and discussion

3.1. Mechanical strength assessment of synthesized supports

Catalysts are regarded as the beating heart of catalytic units in petrochemical industries. In addition to high activity, a reliable catalyst must exhibit resistance to thermal and mechanical stresses, which is achieved through high mechanical strength. All nine synthesized spherical γ-alumina support samples using the oil drop method were evaluated for mechanical strength. Table 2 shows the BET surface area and mechanical strength of supports as responses to the Taguchi M9 array for the preparation of supports. Tables 3 and 4 show the results of the analysis of variance for both responses.

Figure 3 graphically shows the results of Table 2. As can be seen from these graphs and Table 2, the highest mechanical strength of the synthesized supports is associated with the sample that has the lowest pore

volume and therefore the lowest specific surface area (sample 7), and the lowest mechanical strength is related to the sample with the highest pore volume and the specific surface area (sample 5). One of the factors that has a great impact on the mechanical failure of porous solid particles, such as solid catalysts, is the presence of pores in their structure because the concentration of mechanical stresses is greater around the pores and cracks. Therefore, more porous particles usually have lower mechanical strength. However, the higher mechanical strength of sample number 7 could be due to the lower amount of pores in its structure. The lower specific surface area indicates a decrease in pores in the support structure [2,8].

Since a reliable industrial catalyst must possess both high mechanical strength and an acceptable surface for catalytic activities, samples 7 and 5 may not be suitable supports for the preparation of the desired catalyst. Based on the aforementioned criteria, Support sample 3 stands out among the synthesized supports.It demonstrates acceptable mechanical strength (65 MPa) while also exhibiting a relatively good specific surface area (258.5 m^2/g), making it the most reliable support among these 9 synthesized samples.

Table 2. Taguchi M_9 array responses

Sample	Factors and Levels				Responses			
	P_1	P_2	P_3	P_4	BET surface area ($m^2.g^{-1}$)	Mechanical strength (MPa)*	Standard deviation (MPa)**	BJH total pore Volume ($cm^3.g^{-1}$)
1	1.8	4	35	750	240.3	58	8.64	0.105
2	2	8	30	750	229.1	64	9.11	0.101
3	1.8	12	30	650	258.5	65	4.38	0.104
4	1.8	8	40	550	230.5	61	5.43	0.095
5	1.6	4	30	550	304	33	6.12	0.133
6	2	12	35	550	237.1	63	8.11	0.103
7	1.6	12	40	750	224.3	74	3.43	0.102
8	2	4	40	650	256.1	45	7.23	0.122
9	1.6	8	35	650	245.1	53	5.98	0.108

* Arithmetic mean value
** Standard deviation of the mechanical strength data

Table 3. ANOVA results for the BET surface area response

Terms	Sum of Squares	df	Mean square	F-value	p-value	
Model	4612.89	12	922.58	26.31	0.0011	Significant
P_1	14.88	2	14.88	0.4244	0.5612	
P_2	965.95	2	965.95	27.55	0.0135	
P_3	1085.32	2	1085.32	30.96	0.0115	
P_4	105.18	2	791.24	22.57	0.0177	
$P_1 * P_3$	1317.13	4	1317.13	37.57	0.0087	
Lack of fit					0.1816	Not Significant

Adj R-Squared = 0.9406
R^2 = 0.9777 Adeq precision = 16.48
Predicted R^2 =0.8933

3.2. CO conversion assessment of prepared catalysts

After the preparation of the catalysts, the FTS reaction was performed over all nine supported catalysts under the same experimental conditions within the following ranges: temperature 240-300 ℃, pressure 2 bar, H_2/CO molar ratio of 2/1, and GHSV= 3000 h^{-1}. Figure 4 shows the CO conversion of the Fischer-Tropsh reaction on the catalysts made in this work at the investigated temperatures. As seen in Figure 4, the catalyst made on support sample number 3 has a relatively higher CO conversion among other catalysts. Meanwhile, the results of mechanical strength tests showed that support number 3 also had good mechanical strength. Since the mechanical strength of the catalyst is dependent on the strength of its support, the catalyst made on support number 3, in addition to having a high conversion percentage, also had good mechanical strength, and for these reasons, this catalyst was chosen as the selected reliable catalyst among other samples.

3.3. The synthesized catalyst characterization (before and after the FTS reaction)

3.3.1. *The XRD pattern*

Figure 5 illustrates the phases identified by the samples before and after the FTS reaction using XRD patterns.

According to the XRD results, the phase changes of the Fe catalyst in the FTS reaction converted to Fe_2O_3. → Fe_3O_4 → Fe_xO →Fe carbide [24]. The identified phases before the reaction were Fe_2O_3 (Rhombohedral), Fe_3O_4 (cubic), K_2O (cubic), and CuO (monoclinic).

The formation and distribution of carbide phases after the test depend on the reaction conditions. The detected phases formed were characterized by XRD after the test, and these phases are carburized to Fe_2O_3 (rhombohedra), Fe_3O_4 (cubic), FeO (cubic), K_2O (cubic), $KFeO_2$ (cubic), CuO (monoclinic), Fe_3C (orthorhombic), $Fe_{2.5}C$ (monoclinic).

Golestan et al reported that the formation and distribution of the carbide phase can tune the CO activation pathways [25]. Also, Pham et al and Zhang and Schrader concluded that the carbide phase is an activation pathway for the CO dissociation and formation of hydrocarbons.

The presence of somewhat sharp diffraction peaks in the XRD patterns demonstrates the crystallite growth of the synthesized alumina and calcined sample at 650℃ and used the sample after the test reactor. Cu and K phases were rarely identified by XRD test due to their low concentration and dispersion them.

Table 4. ANOVA results for the mechanical strength response

Terms	Sum of Squares	df	Mean square	F-value	p-value	
Model	1034.60	8	258.65	6.66	0.0367	Significant
P_1	1.10	2	1.10	0.0283	0.8745	
P_2	675.99	2	675.99	17.40	0.0140	
P_3	54.68	2	54.68	1.41	0.3011	
P_4	186.09	2	186.09	4.79	0.0938	
Lack of fit					0.1023	Not significant

Adj R-Squared = 0.7388
R^2 = 0.8694 Adeq precision = 8.85
Predicted R^2 =0.3046

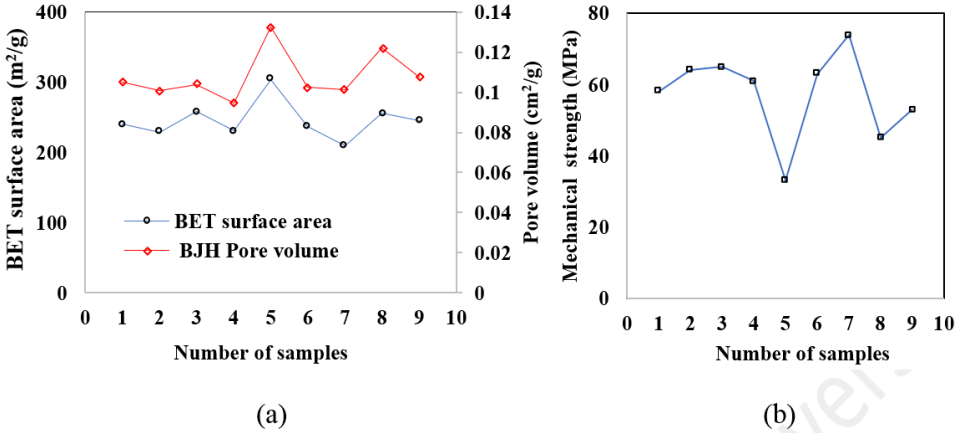

Figure 3. (a) BET surface area, BJH pore volume, and (b) mechanical strength of synthesized γ-Al_2O_3 supports

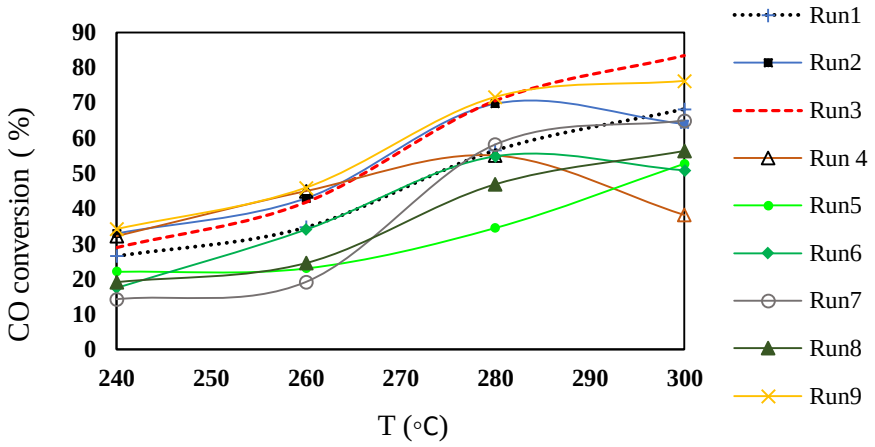

Figure 4. CO conversion of the synthesized catalyst samples in different temperature

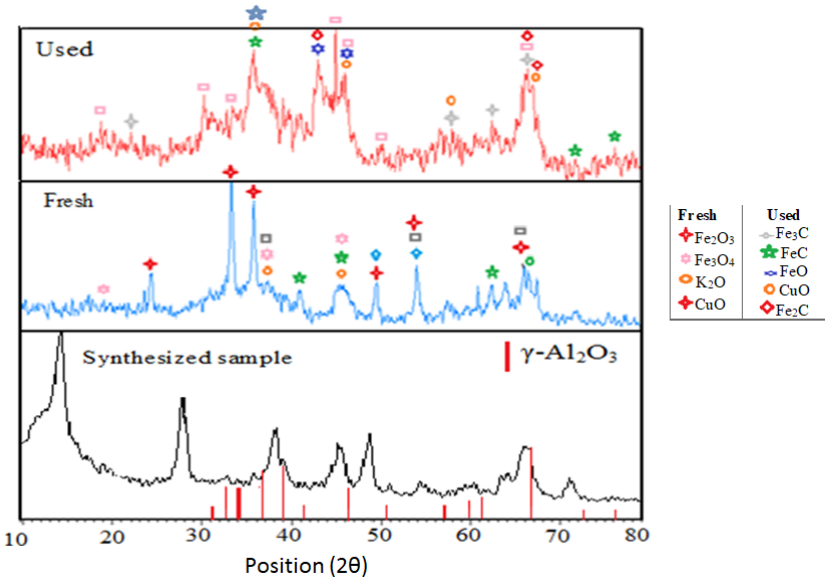

Figure 5. XRD patterns of fresh and used synthesized catalysts containing 100%Fe/0.2K/0.4Cu

3.3.2. *SEM and EDS analysis*

Figure 6a and b show the SEM images of the optimally synthesized γ-Al_2O_3 support with two magnifications. As can be seen in these figures, synthesized γ-alumina support is perfectly uniform and spherical with 1.5 ± 0.2 mm in diameter, and also no evidence of breakage is seen on the surface of the support. However, spherical γ-alumina supports without cracks or defects are important to limit the attrition of catalyst particles and pressure drop in a fixed-bed reactor. The EDX analysis results (Figure 7) indicate a desirable homogeneous loading of the constituent elements within the synthesized catalyst on optimal γ-Al_2O_3 support, including Fe, Cu, K, and Al.

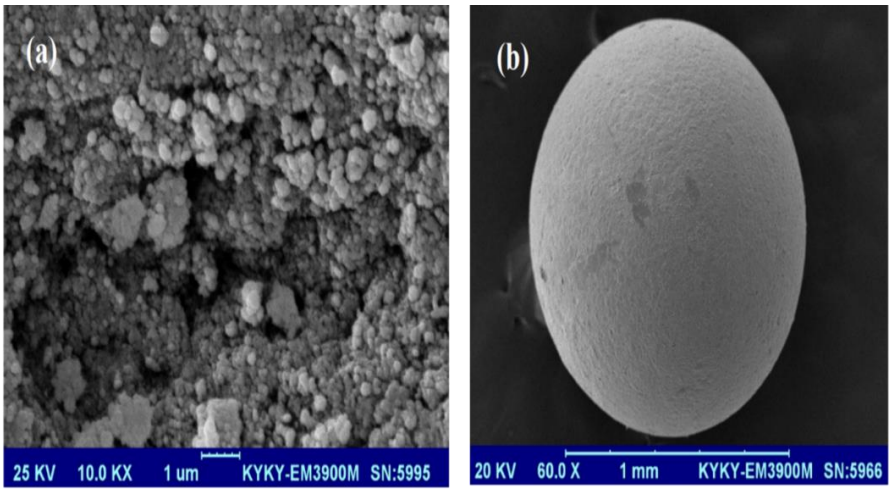

Figure 6. a and b SEM bright area images of the optimal synthesized γ-Al_2O_3 support

3.4. Catalytic performance of the optimized catalyst

As mentioned above, support number 3, among other synthesized supports, exhibited relatively high mechanical strength and an acceptable specific surface area. Considering that the mechanical strength of the support determines the strength of the catalyst, and in addition, the catalyst made on this support had a good catalytic performance in terms of CO conversion, the prepared catalyst on support number 3 was selected as the optimal, reliable catalyst for further research.

In the third step, the performance of this optimal catalyst was evaluated in terms of its CO conversion, C_4 selectivity, and O/P selectivity during the Fischer-Tropsch synthesis (FTS) reaction under various conditions of temperature, pressure, gas hourly space velocity (GHSV), and H_2/CO ratio.

Next, the necessary statistical analyses were performed using historical data in Design Expert. Table 5 shows the investigated variables and obtained results in all runs.

3.4.1. *The Effect of variables on the CO conversion*

Figure 8 shows the effects of variables on the CO conversion of the optimum synthesized catalyst in the FTS reaction. As seen in Figures 8a and 8b, the CO conversion increased significantly with the increase of

the H_2/CO ratio at low pressure and temperature. On the other hand, Figure 8c illustrates that an increase in both temperature and GHSV leads to an enhancement in the CO conversion response. Higher temperatures generally lead to increased CO conversion rates. This is because elevated temperatures enhance the mobility of hydrogen on the catalyst surface, facilitating the reaction [25]. Iron-based catalysts can produce hydrocarbons and oxygenated compounds under different pressures, H_2/CO ratios, and temperatures near 300 ◦C [26].

Table 5. The investigated variables and obtained responses

Trial	Variables				Responses		
	T (◦C)	H_2/CO	GHSV (h^{-1})	P (bar)	C_4 Selectivity (%)	O/P Selectivity(%)	CO Conversion (%)
1	225	1	2100	3	1.95	0.05	22.65
2	225	1	2100	3	1.63	0.05	23.78
3	240	1	2100	6	3.25	0.14	14.05
4	240	1	2100	6	2.84	0.15	24.17
5	270	1	2700	9	1.27	0.05	47.98
6	270	1	2700	9	1.24	0.04	49.99
7	255	1	2700	12	1.46	0.04	59.66
8	255	1	2700	12	1.33	0.04	60.91
9	270	1	3300	6	1.83	0.07	50.85
10	270	1	3300	6	1.77	0.07	57.75
11	270	1	3300	6	1.63	0.04	66.42
12	270	1	3300	6	1.73	0.04	66.66
13	255	1	3300	3	3.10	0.17	35.22
14	240	1	3900	9	3.54	0.15	9.34
15	240	1	3900	9	3.74	0.14	7.95
16	225	1	3900	12	5.17	0.19	4.86
17	225	1	3900	12	5.17	0.22	4.73
18	270	2	3900	3	0.92	0.006	84.93
19	270	2	3900	3	1.32	0.006	64.65
20	240	2	3300	12	1.41	0.024	50.24
21	240	2	3300	12	1.52	0.03	49.33
22	225	2	2700	6	1.67	0.04	41.31
23	255	2	2100	9	1.64	0.03	48.28
24	255	2	2100	9	1.47	0.04	46.71
25	270	3	2100	12	0.43	0.03	40.35
26	270	3	2100	12	0.97	0.03	45.43
27	240	3	2700	3	1.37	0.01	82.72
28	240	3	2700	3	1.56	0.01	79.53
29	225	3	3300	9	1.29	0.03	36.08
30	225	3	3300	9	1.28	0.03	39.38
31	225	3	3900	6	3.62	0.14	32.95
32	225	3	3900	6	2.11	0.089	33.57

3.4.2. *The Effect of variables on the C4 selectivity*

The simultaneous effects of temperature and H_2/CO ratio on the C_4 selectivity response are shown in Figure 9a. It can be observed in this figure that as the temperature increases, the amount of light hydrocarbon increases with a decrease in the H_2/CO ratio. Furthermore, the interaction between temperature and feed ratio has positive effects on C_4 selectivity.

Fe-based FT catalysts have sparked tremendous attention for higher selectivity to light olefins in reactions with lower H_2/CO ratios at higher temperatures**.** Also, these catalysts demonstrate high activity, stability, and high water-gas-shift (WGS) activity at high temperatures for low H_2/CO feed [27]. In Figure 9b, it is shown that a decrease in temperature at higher GHSV leads to an enhancement in C_4 selectivity response. A slight amount of light hydrocarbon was produced at high temperatures and low pressures, as illustrated in Figure 9c. Previous studies have also shown that increasing pressure slows down the rate of polymerization reactions (increasing the length of the carbon chain) relative to chain scission reactions. As a result, the probability of forming lighter products (such as methane and ethane) increases, and the selectivity of C_4 decreases [27].

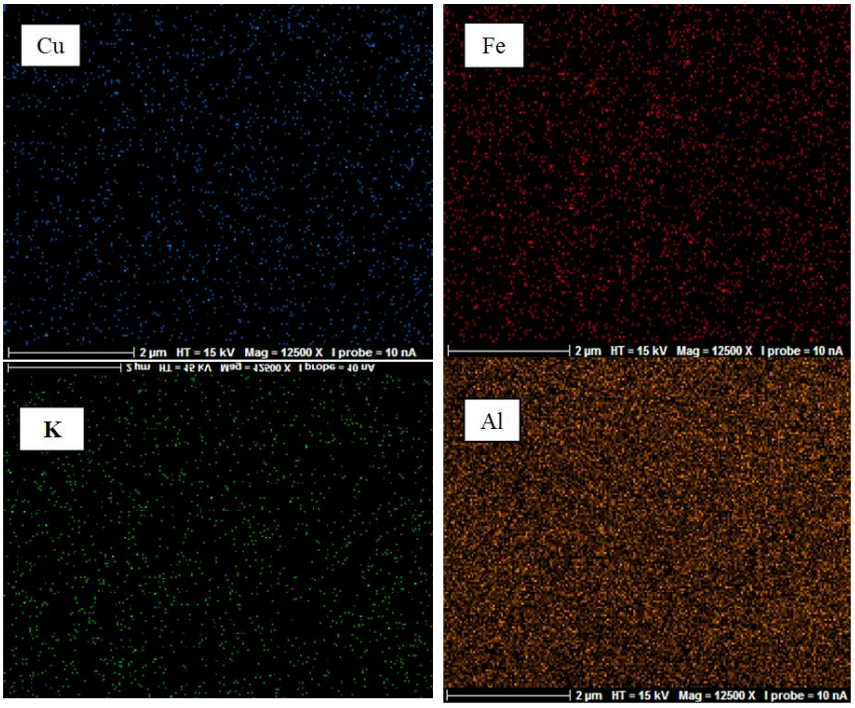

Figure 7. Al, Fe,K and Cu elemental loading of synthesized catalyst on the optimal support

3.4.3. *The Effect of variables on the O/P selectivity*

According to the surface response plots in Figure 10, the effect of molar ratio on the selectivity of O/P depended on temperature (Figure 10a). The higher amount of O/P hydrocarbons was produced at the lower pressure and temperature (Figure 10b). Past research also shows that the lower-temperature FTS process operated between 200 to 400°C, with iron as the catalyst, facilitate the formation of longer hydrocarbon chains. Furthermore, Figure 10c shows that decreasing the pressure while increasing the GHSV increases the production of O/P hydrocarbons.

3.4.4. *Analysis of variance*

The fitness of the CO conversion, C_4, and O/P selectivity models, and the importance of individual terms are specified by analysis of variance (ANOVA). The ANOVA results for all responses are shown in Tables 6**,** 7, and 8. Model terms with a P-value less than 5% confirm their adequacy with 95% confidence intervals. There is only a 0.01% probability for all responses. The R-squared (R^2) values of 0.86, 0.95, and 0.96 for CO conversion, C_4 selectivity, and O/P selectivity models, respectively, demonstrate that the correlation coefficients of the models were undesirable. The "lack-of-fit" test is a proposed statistical model that fits well, so values greater than 0.1(Not significant) are better in all the responses. Adjusted R^2 values will be less than or equal to R^2 values**.** A measure of variation in data by predicted R^2 was the reasonable agreement with the Adjusted R^2 data for all responses. "Adequate precision" is a range of predicted values relative to the average prediction error. In "Adequate precision," ratios of 4 or greater than 4 show adequate model discrimination. The quadratic equations 5 to 7 are presented to fit the experimental data and describe the responses as follows:

$$\text{CO conversion (\%)} = \quad (5)$$
$$38.43 + 13.76\,T + 12.98\,\frac{H_2}{CO} - 4.71\,GHSV + 1.85\,P - 14.00\,T\cdot\frac{H_2}{CO} + 18.49\,GHSV - 11.16\,\frac{H_2}{CO}\cdot GHSV + 14.96\,P^2$$

$$C_4 \text{ selectivity} = \quad (6)$$
$$0.0197 - 00.49\,T - 0.0097\frac{H_2}{CO} + 0.0013\,GHSV - 0.0115\,P + 0.0049\,T\cdot\frac{H_2}{CO} - 0.01948\,T\cdot GHSV - 0.0077\,T\cdot P - 0.0037\,T^2$$

$$O/P \text{ selectivity} = \quad (7)$$
$$0.1271 - 0.0070\,T - 0.0417\,\frac{H_2}{CO} + 0.0275 - 0.0647\,P + 0.1099\frac{H_2}{CO} - 0.1124\,T\cdot GHSV - 0.0467\,T\cdot\frac{H_2}{CO} + 0.0431\,\frac{H_2}{CO}\cdot GHSV - 0.0229\,T^2 + +0.0395\left(\frac{H_2}{CO}\right)^2 - 0.0774\,GHSV^2 - 0.0632\,P^2$$

3.4.5. *Optimization*

Using model graphs and ANOVA, the optimum conditions for the responses were determined. The goal was to maximize CO conversion as well as O/P and C_4 selectivity. The created model demonstrated that the maximum amount of CO conversion was achieved at higher temperature levels. Product selectivity was found to be higher at lower temperatures, particularly when the process was conducted at a low H_2/CO molar ratio and elevated GHSV. According to the results obtained from the models, the temperature shows different behaviors, and low pressure and H_2/CO molar ratio each have positive effects on the products selectivity. An important point is that the parameter levels must be selected based on the optimization objectives.

Table 9 presents the maximum product values and their operating conditions.

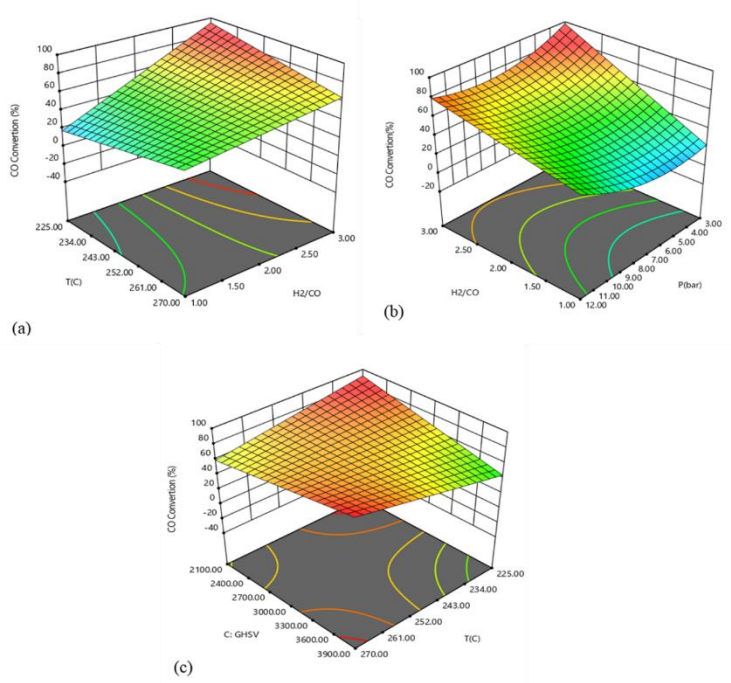

Fiure 8. Response surface 3D plots showing the variation of CO conversion with a) temperature and H_2/CO ratio b) H_2/CO ratio and pressure c) GHSV and temperature

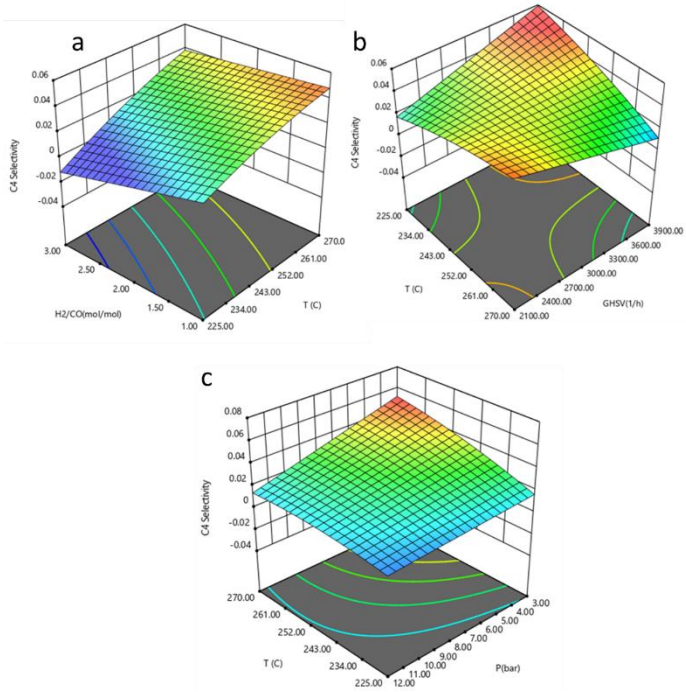

Figure 9. Response surface 3D plots showing the variation of C_4 selectivity with a) temperature and H_2/CO ratio b) temperature and GHSV c) pressure and temperature

4. Conclusions

The oil drop technique has proven to be an effective method for producing spherical γ-Al_2O_3 supports with a consistent size distribution. The optimal support sample, which simultaneously had both suitable surface area and mechanical strength, was obtained under the following operating conditions: an Al/H ratio of 1.8, HMTA solution concentration of 30 wt.%, aging time of 12 hours, and a calcination temperature of 650°C for 4 h. The catalyst made on this optimized support had a good CO conversion in FTS among catalysts made on other supports. After evaluating the reactor performance of this reliable catalyst under various conditions, the necessary statistical analyses were performed. In the temperature range studied in this work, increasing the temperature from 225 to 270 ◦C, especially at low H_2/CO ratios, led to an increase in the CO conversion as well as the C_4 selectivity. Increasing the pressure from 3 to 12 bar led to an increase in the CO conversion while decreasing the selectivity of the products. The operating conditions for the product optimization were obtained as T=270°C, P=3 bar, GHSV=2153.40 h-1, and H2/CO=1.

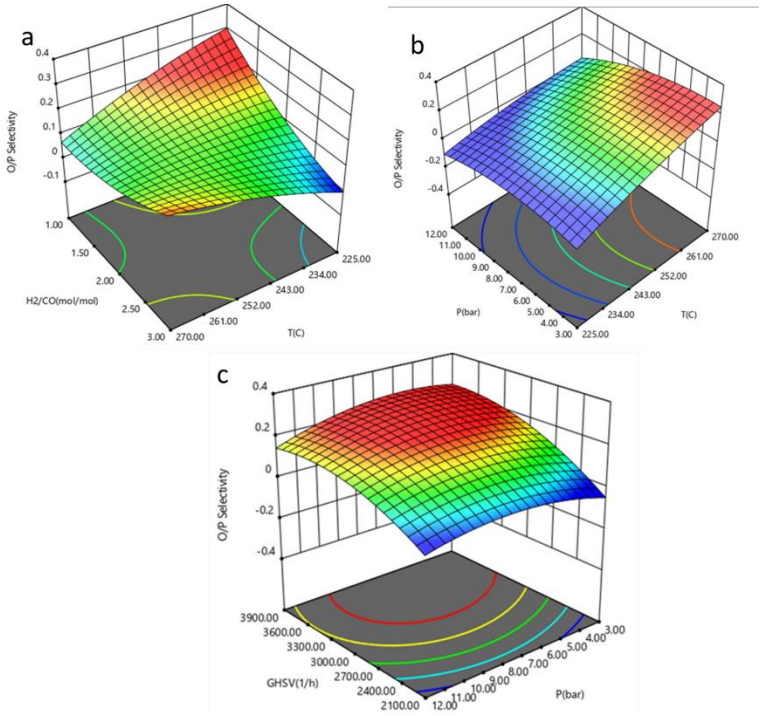

Figure 10. Response surface 3D plots showing the variation of the O/P selectivity with a) temperature and H_2/CO ratio b) temperature and pressure c) pressure and GHSV

Table 6. ANOVA results for the CO conversion response

Terms	Sum of Squares	df	Mean square	F-value	p-value	
Model	12959.63	7	1851.38	22.73	<0.0001	Significant
T	2061.84	1	2061.84	25.31	<0.0001	
H_2/CO	1624.60	1	1624.60	19.94	0.0002	
GHSV	130.36	1	130.36	1.60	0.2180	
P	53.64	1	53.64	0.6585	0.4251	
T* H_2/CO	2592.05	1	2592.05	31.82	<0.0001	
T* GHSV	822.24	1	822.24	10.09	0.0041	
$(H_2/CO)^2$	1538.42	1	1538.42		0.0002	
Lack of fit	1494.99	8	186.87	6.50	0.1608	Not Significant

Adj R-Squared = 0.8307
Adeq precision = 16.92
Predicted R2 =0.7482

Table 7. ANOVA results for the C_4 selectivity response

Terms	Sum of Squares	df	Mean square	F-value	p-value	
Model	0.0042	8	0.0005	53.08	<0.0001	Significant
T	0.0004	1	0.0004	38.49	<0.0001	
H_2/CO	0.0015	1	0.0015	149.85	<0.0001	
GHSV	0.0009	1	0.0009	0.9224	0.3011	
P	0.0008	1	0.0008	81.44	<0.0001	
T* H_2/CO	0.0003	1	0.0003	30.12	<0.0001	
T* GHSV	0.0013	1	0.0013	132.73	<0.0001	
T*P	0.0002	1	0.0002	20.94	0.0128	
T^2	0.0001	1	0.0001	7.28		
Lack of fit	0.0001	7	0.000	1.10	0.4094	Not Significant

Adj R-Squared = 0.9308
Adeq precision = 28.16
Predicted R2 =0.8850

Table 8. ANOVA results for the O/P selectivity response

Terms	Sum of Squares	df	Mean square	F-value	p-value	
Model	0.1088	8	0.0084	31.15	<0.0001	Significant
T	0.0001	1	0.0001	0.2472	0.6251	
H_2/CO	0.0070	1	0.0070	26.24	<0.0001	
GHSV	0.0014	1	0.0014	5.31	0.0333	
P	0.0131	1	0.0131	48.62	<0.0001	
T* H_2/CO	0.0052	1	0.0052	19.41	0.0003	
T* GHSV	0.0175	1	0.0175	65.29	<0.0001	
T*P	0.0061	1	0.0061	22.85	0.0001	
H_2/CO* GHSV	0.0024	1	0.0024	8.76	0.0084	
GHSV*P	0.0014	1	0.0014	5.17	0.0355	
T^2	0.0022	1	0.0022	8.25	0.0101	
$(H_2/CO)^2$	0.0038	1	0.0038	14.25	0.0014	
$(GHSV)^2$	0.0027	1	0.0027	10.01	0.0054	
P^2	0.0038	1	0.0038	14.28	0.0014	
Lack of fit	0.0015	2	0.0008	3.71	0.2474	Not Significant

Adj R-Squared = 0.9267
Adeq precision = 18.07
Predicted R2 =0.8457

Table 9. Operating conditions for obtaining maximum responses

Products	T (◦C)	P (bar)	H_2/CO	GHSV (h^{-1})	Maximum values	
CO Conversion (%)	241.3	3	3	2621.8	61.9	
C_4 Selevtivity (%)	225.2	12	1.1	3896.2		4.1
O/P Selectivity (%)	241.6	3.1	1.1	3750.6		0.2

Acknowledgments

This article is dedicated to the memory of our dear professor, Hossein Atashi, who passed away during the writing of this article. He was a remarkable individual who made significant contributions to this field through his valuable research.
The authors would also like to express their deepest gratitude to everyone who supported and assisted them in conducting this research. Special thanks go to the personnel of Bouali Sina Petrochemical Company (BSPC), located in Iran, south of the Persian Gulf, for their invaluable assistance.

Authors Contribution
All authors have contributed equally to prepare the paper.

Availability of data and materials
The data that support the findings of this study are available from the corresponding author, upon reasonable request.

Conflict of interests
The authors declare that they have no known competing financial interests or personal relationships that could have appeared to influence the work reported in this paper.

References

[1] M. Abdollahi, H. Atashi, F.F. Tabrizi, Adv. Powder Technol. 28 (2017) 1356-1371.
DOI: https://doi.org/10.1016/j.apt.2017.03.004

[2] M. Zakeri, A. Samimi, M. Khorram, H. Atashi, A.A. Mirzaei, Powder Technol. 200 (2010) 164-170.
DOI: https://doi.org/10.1016/j.powtec.2010.02.021

[3] Y. Chen, J. Wei, M. S. Duyar, V. V. Ordomsky, A.Y. Khodakov, J. Liu, Chem. Soc. Rev. 50 (2021) 2337-2366.
DOI: https://doi.org/10.1039/D0CS00905A

[4] M. Amin, M. Usman, T. Kella,W. Ullah Khan, I. Afzal Khan, K. H. Lee, Front. Chem. 12 (2024) 1462503.DOI: https://doi.org/10.3389/fchem.2024.1462503

[5] M. Amin, S. Munir, N. Iqbal, S. M. Wabaidur, A. Iqbal, Catal. 12 (2022) 1234.
DOI: https://doi.org/10.3390/catal12101234

[6] Z. Yang, Y. Lin, Ind. Eng. Chem. Res. 39 (2000) 4944-4948.
DOI: https://doi.org/10.1021/ie000562r

[7] A. Samimi, M. Zakeri, B. Maleki, D. Mohebbi-Kalhori, Particuology. 21 (2015) 74-81.
DOI: https://doi.org/10.1016/j.partic.2014.10.002

[8] M. Zakeri, A. Samimi, M. Shafiee Afarani, A. Salehirad, Part. Sci. Technol. 36 (2018) 96-103.
DOI: https://doi.org/10.1080/02726351.2016.1220437

[9] J. Choi, J. Kim, K. Sang Yoo, T. Gyu Lee, Powder Technol. 181 (2008) 83-88.
DOI: https://doi.org/10.1016/j.powtec.2007.06.022

[10] S. Sathish, M. Geetha, A. Udayakumar, S. Senthil Kumar, R. Asokamani, Trans. Indian. Inst. Met. 65 (2012) 485-490.
DOI: https://doi.org/10.1007/s12666-012-0158-1

[11] G. Bertrand, P. Roy, C. Filiatre, C. Coddet, Chem. Eng. Sci. 60 (2005) 95-102.
DOI: https://doi.org/10.1016/j.ces.2004.04.042

[12] P. M. Arvela, I. Simakova, Z. Vajglová, N. Kumar, D. Yu. Murzin, Catal. Today. 423 (2023) 113933.
DOI: https://doi.org/10.1016/j.cattod.2022.10.015

[13] M. Zakeri, A. Samimi, M. S. Afarani, A. Salehirad, Particuology. 32 (2017) 160-166.
DOI: https://doi.org/10.1016/j.partic.2016.08.006

[14] A. Islam, Y. H. Taufiq-Yap, C. M. Chu, E. S Chan, P. Ravindra, J. Porous Mater. 19 (2012) 807-817.
DOI: https://doi.org/10.1007/s10934-011-9535-0

[15] B. H. Davis, Catal. Today. 71 (2002) 249-300.
DOI: https://doi.org/10.1016/S0920-5861(01)00455-2

[16] S. Deng, Y. Lin, AIChE J. 43 (1997) 505-514.
DOI: https://doi.org/10.1002/aic.690430223

[17] Z. Zhang, J. Zhang, X. Wang, R. Si, J. Xu, Y. F. Han, J. Catal. 365 (2018) 71-85.
DOI: https://doi.org/10.1016/j.jcat.2018.05.021

[18] T. N. Phaahlamohlaka, M. W. Dlamini, M. W. Mogodi, D. O. Kumi, L. L. Jewell, D. G. Billing, N. J. Coville, Appl. Catal. A-Gen. 552 (2018) 129-137.
DOI: https://doi.org/10.1016/j.apcata.2017.12.015

[19] C.L. Tucker, E. van Steen, Catal. Today. 342 (2020) 115-123.
DOI: https://doi.org/10.1016/j.cattod.2018.12.049

[20] M. Oschatz, N. Krans, J. Xie, K. P. de Jong, J. Energy Chem. 25 (2016) 985-993.
DOI: https://doi.org/10.1016/j.jechem.2016.10.011

[21] T.T. Lari, A.A. Mirzaei, H. Atashi, RSC Adv. 7 (2017) 34497-34507.
DOI: https://doi.org/10.1039/C7RA05490D

[22] M. Mansouri, H. Atashi, M. M. Khalilipour, N. Setareshenas, F. Shahraki, J. Korean Chem. Soc. 57 (2013) 769-777.
DOI: https://doi.org/10.5012/jkcs.2013.57.6.769

[23] P. Müller, A. Russell, J. Bergstedt, J. Tomas, Granul. Matter. 18 (2016) 1-14.
DOI: https://doi.org/10.1007/s10035-016-0610-8

[24] A.A. Adeyiga, Development of attrition resistant iron-based Fischer-Tropsch catalysts, Hampton University, 2003. (US)

[25] H. Atashi, F. Rezaeian, Int. J. Hydrogen Energy. 42 (2017) 15506.
DOI: https://doi.org/10.1016/j.ijhydene.2017.04.224

[26] T. Fu, Y. Jiang, J. Lv, Z. Li, Fuel Process. Technol. 110 (2013) 141-149.
DOI: https://doi.org/10.1016/j.fuproc.2012.12.006

[27] Z. Teimouri, N. Abatzoglou, A.K. Dalai, J. Fuels 360 (2024) 130512.
DOI: https://doi.org/10.1016/j.fuel.2023.130512